

# Extracellular matrix 1 (ECM1) regulates the actin cytoskeletal architecture of aggressive breast cancer cells in part via S100A4 and Rho-family GTPases

P. Gómez-Contreras<sup>1</sup> · J. M. Ramiro-Díaz<sup>5</sup> · A. Sierra<sup>2</sup> · C. Stipp<sup>3</sup> · F. E. Domann<sup>4</sup> · R. J. Weigel<sup>1</sup> · G. Lal<sup>1</sup>

Received: 24 March 2016 / Accepted: 12 October 2016 / Published online: 21 October 2016  
© Springer Science+Business Media Dordrecht 2016

**Abstract** ECM1 overexpression is an independent predictor of poor prognosis in primary breast carcinomas, however the mechanisms by which ECM1 affects tumor progression have not been completely elucidated. ECM1 was silenced in the triple-negative breast cancer cell lines Hs578T and MDAMB231 using siRNA and the cells were evaluated for changes in morphology, migration, invasion and adhesion. Actin cytoskeleton alterations were evaluated by fluorescent staining and levels of activated Rho GTPases by pull down assays. ECM1 downregulation led to significantly diminished cell migration ( $p = 0.0005$  for Hs578T and  $p = 0.02$  for MDAMB231) and cell adhesion ( $p < 0.001$  for Hs578T and  $p = 0.01$  for MDAMB231). Cell invasion (matrigel) was reduced only in the Hs578T cells ( $p < 0.01$ ). Silencing decreased the expression of the prometastatic molecules S100A4 and TGF $\beta$ R2 in both cell lines and CD44 in Hs578T cells. ECM1-silenced cells also

exhibited alterations in cell shape and showed bundles of F-actin across the cell (stress fibers) whereas NT-siRNA treated cells showed peripheral membrane ruffling. Downregulation of ECM1 was also associated with an increased F/G actin ratio, when compared to the cells transfected with NT siRNA ( $p < 0.001$  for Hs578T and  $p < 0.00035$  for MDAMB231) and a concomitant decline of activated Rho A in the Hs578T cells. Re-expression of S100A4 in ECM1-silenced cells rescued the phenotype in the Hs578T cells but not the MDAMB231 cells. We conclude that ECM1 is a key player in the metastatic process and regulates the actin cytoskeletal architecture of aggressive breast cancer cells at least in part via alterations in S100A4 and Rho A.

**Keywords** ECM1 · Metastasis · Actin cytoskeleton · Rho A · S100A4

**Electronic supplementary material** The online version of this article (doi:10.1007/s10585-016-9827-5) contains supplementary material, which is available to authorized users.

✉ G. Lal  
Geeta-lal@uiowa.edu

<sup>1</sup> Division of Surgical Oncology and Endocrine Surgery, Department of Surgery, University of Iowa, 200 Hawkins Drive, 4641 JCP, Iowa City, IA 52242, USA

<sup>2</sup> Department of Internal Medicine, University of Iowa, Iowa City, IA, USA

<sup>3</sup> Department of Biology, University of Iowa, Iowa City, IA, USA

<sup>4</sup> Free Radical and Radiation Biology, University of Iowa, Iowa City, IA, USA

<sup>5</sup> Department of Physiology, Georgia Regents University, Augusta, GA, USA

## Background

Extracellular matrix 1 (ECM1) overexpression characterizes a number of epithelial malignancies including invasive ductal breast carcinomas, esophageal squamous cell carcinomas, gastric cancers, colorectal, lung, laryngeal, hepatocellular, biliary and thyroid cancers [1–6]. Studies have suggested an association between ECM1 overexpression, increased metastasis and poor prognosis in several types of cancers, including breast carcinoma, laryngeal, hepatocellular, gastric and cholangiocarcinomas [5–10].

We have previously demonstrated, in a consecutive cohort of 150 patients with invasive breast cancer, that ECM1 over-expression is an independent marker of worse disease-specific and disease-free survival [11]. However, the intracellular mechanisms responsible for the effects of

ECM1 on outcomes have not been fully elucidated. Interestingly, ECM1 transgenic mice do not appear to have a cancer predisposition, suggesting that ECM1 plays a role in tumor progression, rather than initiation [12]. In keeping with this, ECM1 has been reported to promote angiogenesis and its expression appears to correlate with increased cell division [4, 5, 7]. Additional evidence indicates that ECM1 overexpression increases lymphatic and microvessel density [8] as well as cellular proliferation and drug resistance to trastuzumab via activation of epidermal growth-factor signaling [13]. Furthermore, ECM1 overexpression is associated with maintenance of the cancer stem cell (CSC) phenotype and with the progression of the epithelial to mesenchymal (EMT) transition [14].

Sercu et al. [15] postulated that the binding of ECM1 to components of the dermal-epidermal junction *in vivo* may act as a “biological glue” in the framework of normal skin where it is highly expressed. As such, one hypothesis is that ECM1 expression affects tumor cell characteristics and as a consequence, metastatic potential. In fact, our group has also demonstrated that downregulation of ECM1 reduced attachment of melanoma cells to a plastic surface [16]. Additionally, other studies demonstrate that knocking down ECM1 suppresses migration and invasion of cholangiocarcinoma and breast cancer cell lines [6, 14].

The purpose of the current study is to further investigate the intracellular mechanisms by which ECM1 overexpression regulates metastatic behavior using aggressive breast cancer cell lines. Our results demonstrate that ECM1 affects cellular shape and morphology, in addition to migration, invasion and attachment in breast cancer cells. In addition, these changes in cell morphology are associated with alterations in actin stress fiber formation and increased F/G-actin ratio. We also show that these events are likely mediated by the Rho GTPase pathway and Rho A, in particular. Lastly, our results indicate that ECM1 regulates the expression of other genes known to be involved in metastatic process, most notably S100A4, TGF $\beta$ R2 and CD44; and that S100A4 is the likely effector of the observed actin cytoskeletal changes. Taken together, our novel findings support the central role for ECM1 in the metastatic process and enhance our knowledge regarding the multitude of pathways by which this may occur.

## Methods

### Cell culture

Hs578T and MDAMB231 cell lines were purchased from ATCC (American Type Culture Collection, Manassas, VA, USA) and have been shown to express ECM1 in previous studies from our lab [17]. Cells were grown in D-MEM

medium (GIBCO/BRL, Grand Island, NY, USA) supplemented with 10 % Fetal Bovine Serum (FBS), L-glutamine (2 mM), penicillin (100 U/ml), streptomycin (100 mg/ml) (D-MEM supplemented) and incubated at 37 °C in 5 % CO<sub>2</sub>/95 % air.

### RNA interference

Cells were seeded in Costar six well plates (Corning, NY, USA). After reaching 50 % confluence, culture media was substituted with Opti-MEM (GIBCO/Life Technologies, Carlsbad, CA, USA). Cells were transfected with interference RNA (siRNA) [ECM-1 Silencer Select Pre-designed siRNA, 100–200 nM, targeting exon 6, ECM-1 Silencer Select Pre-designed siRNA, 100–200 nM, targeting exon 2, S100A4 Silencer Select Pre-designed siRNA, 100–200 nM, (Ambion/Life Technologies, Carlsbad, CA, USA)] using Lipofectamine RNAiMAX (Invitrogen/Life Technologies, Carlsbad, CA, USA). Silencer Select Negative Control #1 siRNA (Ambion/Life Technologies, Carlsbad, CA, USA) was used as control siRNA. Adequate downregulation was assessed by western blotting.

### Western blotting

Antibodies used were as follows: Anti-ECM-1, C-12 (Santa Cruz Biotechnology, Santa Cruz, CA, USA), anti-CD44, 2C5 (R&D systems, Minneapolis, MN, USA), anti-TGF $\beta$ R2, L-21 (Santa Cruz Biotechnology, Santa Cruz, CA, USA), anti S100A4, A-7 (Santa Cruz Biotechnology, Santa Cruz, CA, USA), anti Rho C, D40E4 (Cell Signaling, Beverly, MA, USA), anti Rho A, 67B9 (Cell Signaling, Beverly, MA, USA), anti GAPDH, 6C5 (Santa Cruz Biotechnology, Santa Cruz, CA, USA),  $\beta$ -actin monoclonal antibody, AC-74 (Sigma-Aldrich, Saint Louis, MO, USA), goat anti-Rabbit HRP secondary antibody (Cell Signaling, Beverly, MA, USA) and Goat anti-mouse HRP secondary antibody (Santa Cruz Biotechnology, Santa Cruz, CA, USA).

For the blots, denatured and reduced protein lysate were loaded, resolved by NuPAGE Bis-Tris 10 % gels (Invitrogen/Life Technologies, Carlsbad, CA, USA), and transferred to an Amersham Hybond-ECL nitrocellulose membrane (GE Healthcare Bio-Sciences Corp, Piscataway, NJ, USA). Membranes were blocked with a suspension of 5 % fat-free milk powder in 20 mM Tris, 137 mM NaCl, 3 mM KCl and 0.1 % Tween-20 pH 7.6 (TBS-T). The membranes were incubated for 1 h with the respective antibody diluted in milk 2 %-TBS-T, washed thrice in TBS-T and incubated for 1 h with respective peroxidase antibody diluted 1:3000 in milk 2 %-TBS-T. Membranes were developed with ECL plus western blotting detection system and exposed to an Amersham Hyperfilm ECL film (both from GE Healthcare Bio-Sciences Corp, Piscataway,

NJ, USA). Membranes were also incubated with anti GAPDH antibody 1:1000 to confirm loading quality. Blots were repeated at least three times to confirm changes and perform densitometry analyses.

### Wound healing migration assay, invasion assay and adhesion assay

These functional studies were performed as previously described [17]. For wound healing, the cell monolayer was scratched with a 200  $\mu$ l pipette tip. Plates were washed to remove floating cells and incubated with D-MEM (supplemented) overnight. Migrating cells from the edge of the wound were photographed at various time points until closure using an Olympus IX51 Inverted Fluorescence Microscope and Digital Camera. Percentage of open/healed wound area was calculated using T-Scratch software [18]. Invasion was assessed using BD BioCoat™ Matrigel™ Invasion Chambers (BD Biosciences, Bedford, MA, USA). Briefly, cells were detached from the culture plates using 0.6 mM EDTA, washed and re-suspended in D-MEM media without supplements. A total of 0.5 ml of cell suspension at 500,000 cells/ml were added to each insert and incubated for 24 h, at 37 °C, 5 % CO<sub>2</sub>. Non-invading cells were cleaned from the upper surface of the insert by scrubbing with a cotton swab. The inserts were incubated with 0.5 ml of thiazolyl blue tetrazolium bromide (MTT) solution (Sigma-Aldrich, Saint Louis, MO, USA) at 0.5 mg/ml and dissolved in culture media (without supplements) and phenol red for 1 h at 37 °C. After staining, the membranes were collected from the inserts, and MTT dye was dissolved with dimethyl sulfoxide (DMSO). MTT concentration was determined measuring its absorbance at 550 nm and considered as an index of the number of invaded cells. For adhesion, cells were detached with EDTA 0.6 mM, centrifuged and resuspended in complete culture media. Twelve-well plates were seeded in triplicate with 50,000 cells/well. The cells were incubated at 37 °C, 5 % CO<sub>2</sub> for 2 h. The supernatant was discarded and the cells were stained with MTT solution at 0.5 mg/ml in RPMI-1640. A total of 250  $\mu$ L of DMSO was added per well prior to evaluating absorbance at 550 nm.

### Morphology assessment and Immunofluorescence

Cells were fixed in 4 % paraformaldehyde for 15 min, washed in PBS, permeabilized with 0.2 % Triton-X 100 in PBS for 8 min, and blocked with 2.5 % bovine serum albumin in PBS for 30 min at room temperature. To determine the levels of F-actin and G-actin, the cells were incubated with Phalloidin 568 (Life Technologies, Grand Island, NY, USA) + Alexa-DNaseI 488 (Life Technologies, Grand Island, NY, USA) at 1:50 and 1:100 dilution respectively, for 1 h at room

temperature. The cells were washed with PBS and mounted in Vectashield + DAPI (Vector Labs, Burlingame, CA, USA). The cells were visualized using a confocal microscope ( $\lambda$  excitation emission) (Zeiss LSM 710, Germany) at the University of Iowa, Central Microscopy Core.

Levels of actin were quantified as follows. Using the confocal program Zen, multiple rectangular regions of interest (ROI) were drawn on each cell to cover the entire cell surface excluding the nucleus. The integrated intensity per pixel for each dye on each ROI was calculated and averaged to obtain the intensities of F- and G-actin staining in the whole cell. The procedure was repeated for all the cells in the field and the average intensity for each dye was used to determine the ratio F-actin/G-actin [19].

### Pull down assays

Rho A and Rho C activity was determined as previously described [20]. In brief 5  $\times$  10<sup>6</sup> cells were plated in 150 mm dishes and cultured to achieve about 30 % confluence. After 96 h of siECM1 treatment, the cells were lysed with 800  $\mu$ l of ice cold PhosphoSafe Novagen lysis buffer (Millipore, Billerica, MA, USA) with protease inhibitors and the supernatant was centrifuged at 10,000 $\times$ g for 1 min at 4 °C. Protein quantification was performed by PIERCE BCA Protein assay (Thermo Scientific, Rockford, IL, USA). Lysates for each condition were snap frozen until use. Active GTPase was determined using 30  $\mu$ g of Rhotekin-RBD protein GST Sepharose beads or PAK-GST Protein beads (Cytoskeleton Inc, Denver, CO, USA) per 500  $\mu$ g/ml of protein lysates for each experimental condition mixed for 1 h at 4 °C, resolved in SDS-PAGE and blotted with their respective antibodies. Lysates of HeLa cells (70 % confluence) were used as positive and negative controls. For the positive control, the lysate was activated with GTP-alpha-s (Cytoskeleton Inc, Denver, CO, USA) and with GDP (Sigma Aldrich, St Louis, MO, USA) for the negative control. After 15 min of incubation the reaction was stopped with MgCl<sub>2</sub> (Ambion, Life technologies, Austin, TX, USA) and the lysates were resolved as described above.

### Expression of metastasis-associated genes

The effects of ECM1 downregulation was examined using the TaqMan Human Tumor Metastasis array (Life technologies, Carlsbad, CA, USA) in the Hs578T cell line. Total RNA was extracted after homogenization of cells and tissues using RNeasy mini kit (Qiagen Sciences, Maryland, MD, USA). Total RNA (1  $\mu$ g) was reverse transcribed with the High Capacity cDNA Reverse Transcription Kit (Applied Biosystems, Foster City, CA, USA). The cDNA reaction was diluted to 1:10 and used as a template for real-

time RT-PCR. The cycling conditions were as follows: one cycle of 2 min at 50 °C, one cycle of 10 min at 95 °C, 40 cycles of denaturation (15 s at 95 °C) and annealing/extension (1 min at 60 °C). All reactions were carried out in the Step One Plus Real-Time PCR Systems Thermocycler (Applied Biosystems, Foster city, CA, USA) in duplicate and repeated at least twice. The  $\Delta C_t$  for mRNA expression was calculated relative to the  $C_t$  (threshold cycle) of 18S ribosomal RNA. Relative mRNA expression was calculated using the formula  $2^{-\Delta\Delta C_t}$ . The results obtained were analyzed following the manufacturer protocols. The arrays were run in duplicate on cells transfected with NTsiRNA or ECM1 siRNA. Alterations in RNA expression were confirmed by western blotting.

### S100A4 transfection

Approximately 48 h after ECM1 silencing, S100A4 (GFP-tagged) pCMV6-AC-GFP vector (OriGene Tech, Inc, Rockville, MD, USA) at 0.5  $\mu\text{g/ml}$ , and a control GFP-empty vector (OriGene Tech, Inc, Rockville, MD, USA) were transfected into the cells using Lipofectamine 2000 (Life Technologies, Grand Island, NY, USA). Both vectors and Lipofectamine 2000 were constituted in OptiMEM (Life Technologies, Grand Island, NY, USA) and regular culture media was added after 5 h. Following 48 h of transfection, (96 h after siECM1) the coverslips were rinsed with PBS, fixed with paraformaldehyde (4 % in PBS) for 15 min, washed, permeabilized in PBS + 0.2 % Triton-X 100 for 8 min and blocked with PBS + 2.5 % bovine serum albumin for 30 min at room temperature. The cells were then incubated with Phalloidin 568 (Life Technologies, Grand Island, NY, USA), in the recommended dilution for 1 h at room temperature, washed with PBS and mounted in Vectashield + DAPI (Vector Labs, Burlingame, CA, USA). The cells were visualized using a confocal microscope as described above.

### Statistical analyses

All data are presented as mean  $\pm$  SD. Statistical tests were performed using the SPSS statistical software. Differences between groups were compared using t tests. p values  $\leq 0.05$  were considered statistically significant.

## Results

### ECM1 affects cancer cell migration, invasion and adhesion

The effects of altering ECM1 expression on cellular characteristics important in the metastatic process were examined by

silencing ECM1 using siRNA. Down regulation of ECM1 led to reduced cell migration and delayed wound closure in both breast cancer cell lines (Hs578T and MDAMB231) (Fig. 1a) at 24 h after wounding. The quantification of cell migration using T-scratch software showed a significant diminution in the normalized closed/healed wound area in cells treated with ECM1 siRNA compared with non-targeting (NT) siRNA, ( $p < 0.0005$  for Hs578T and  $p = 0.02$  for MDAMB231) (Fig. 1b). Since ECM1 can affect cell proliferation [14] we repeated the wound assay in MDAMB231 cells following treatment with Mitomycin C (5  $\mu\text{g/ml}$ ) for 2 h. Untreated cells continued to demonstrated a significant reduction in the normalized healed wound area after ECM1-silencing ( $p = 0.01$ ). Cells treated with Mitomycin C showed delayed closure in the NT cells compared to untreated cells ( $p = 0.03$ ). In addition, although there was a trend towards reduced migration in the ECM1 silenced treated cells compared to NT treated cells ( $p = 0.2$ ), it did not reach statistical significance, suggesting that observed ECM1 related differences in wound migration rates may be related to its effects on both cell migration and proliferation (Supplemental Figure 1).

We also found that knocking down ECM1 expression was associated with a significant reduction in cell adhesiveness, as evaluated by cell attachment to a plastic surface ( $p < 0.001$  for Hs578T and  $p = 0.01$  for MDAMB231) (Fig. 2a). In contrast, an ECM1-mediated reduction in cell invasiveness through Matrigel was observed in the Hs578T cell line ( $p < 0.002$ ) but not in the MDAMB231 cell line (Fig. 2b). Taken together, these data suggest that ECM1 down regulation may affect the metastatic capacity of both cell lines through diminishing cell migration, invasion and adhesion.

### ECM1 regulates the expression of other metastasis-associated genes

The metastatic process is complex and the metastasizing phenotype acquired by cells cannot be explained by alteration of a single gene. Therefore, we examined the effects of ECM1 downregulation on the expression of other well-known metastasis-associated genes. Real-time RT-PCR data from the human metastasis array obtained from the Hs578T cell line was normalized by the housekeeping gene hypoxanthine phosphoribosyltransferase 1 (HPRT1). The array was examined for genes showing at least fourfold change in RNA expression (either up or downregulation), when compared with the expression of multiple different housekeeping genes, following ECM1 silencing. Changes in gene expression were confirmed at the level of protein expression by western blotting in both cell lines to evaluate whether they were ECM1-related or cell-line related. Genes with low baseline expression or high standard deviations on the array were excluded from additional western blot analyses.



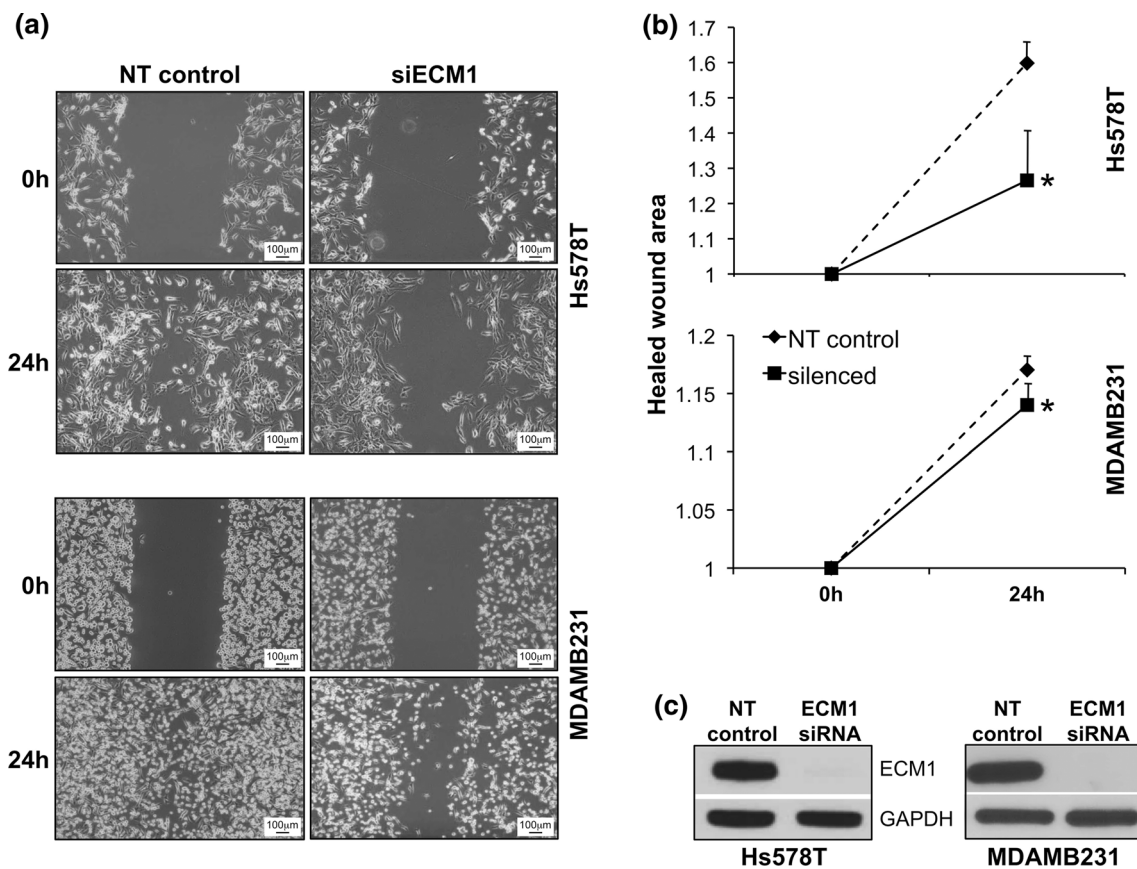


**Fig. 1** Cell migration is diminished after ECM1 knockdown. **a** Wound scratch was performed 72 h after ECM1 silencing (0 h) and images from the same area were taken at  $\times 10$  magnification at 0 and 24 h. **b** A set of four pictures from three independent experiments were analyzed using T-Scratch software. Percentage of healed wound

As shown in Fig. 3a, among the genes showing fourfold reduction at the RNA level, ECM1 downregulation was associated with a concomitant diminution of S100A4 and TGF $\beta$ R2 protein expression in both cell lines. Genes with less than fourfold change but of known relevance to breast carcinogenesis, such as CD44, also appeared to have lower protein expression. Densitometry analyses confirmed significantly reduced S100A4 ( $p = 0.006$  for Hs578T,  $p = 0.02$  for MDAMB231) and TGF $\beta$ R2 ( $p = 0.02$  for Hs578T,  $p = 0.005$  for MDAMB231) expression in both cell lines over multiple experiments. CD44 expression was also significantly diminished in the Hs578T cell line by densitometry ( $p = 0.001$ ) but not in the MDAMB231 cells, as shown in Fig. 3b. Similar results were obtained following ECM1 silencing with an alternate siRNA (data not shown).

### Alterations in cell shape are mediated by changes in actin cytoskeleton

During the metastatic process, cancer cells undergo dramatic molecular and cellular changes by remodeling their cell-cell,

area was normalized by setting the value at 0 h as 1. Statistically significant reduction in the normalized healed wound area was found in both cell lines after ECM1 knockdown ( $*p = 0.0005$  for Hs578T and  $*p = 0.02$  for MDAMB231). Error bars represent SEM. **c** Western Blot data showing ECM1 silencing

cell-matrix interactions and their cytoskeleton [21]. Cytoskeletal remodeling is especially relevant because it can affect not only cell shape but also gene expression through the regulation of the translocation of nuclear factors in different cell lines [22–24]. In our experiments, loss of ECM1 was also associated with changes in the cellular shape, wherein ECM1 siRNA treated cells appeared more elongated and spindle shaped when compared to cells treated with NT siRNA. These alterations were apparent 48 h after ECM1 downregulation and persisted up to 120 h after. Due to the altered morphology noted after ECM1 silencing, we sought to examine changes in the actin cytoskeleton using confocal microscopy staining for globular monomeric G-actin and filamentous polymerized F-actin. As shown in Fig. 4a, changes in cell shape associated with alterations in actin organization were observed in both cell lines after ECM1 silencing. Cells treated with NT siRNA tended to have peripherally organized F-actin with ruffling noted, whereas cells treated with ECM1 siRNA showed bundles of F-actin across the cell, in keeping with the appearance of stress fibers.

**Fig. 2** Attachment and invasiveness are impaired by ECM1 knockdown. **a** Cell attachment to a plastic surface assay was evaluated (in quadruplicate) after 96 h of ECM1 silencing. ECM1 decreased cell attachment ability in both cell lines (\* $p < 0.001$  for Hs578T and  $p = 0.01$  for MDAMB231). **b** Matrigel invasion assay was performed after 72 h of ECM1 silencing. Invasiveness was significantly reduced by ECM1 knockdown in the Hs578T cell line only (\* $p < 0.01$ ). Bars represent SD of the mean for one representative set of experiments which were performed at least three times. Absorbance was measured at 550 nm and serves as a marker of cell number

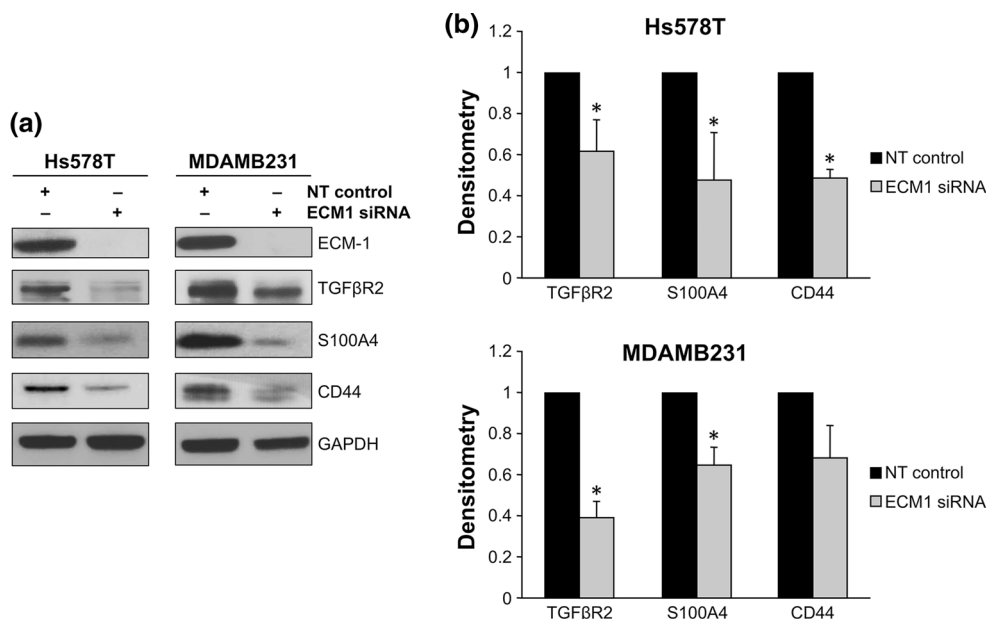
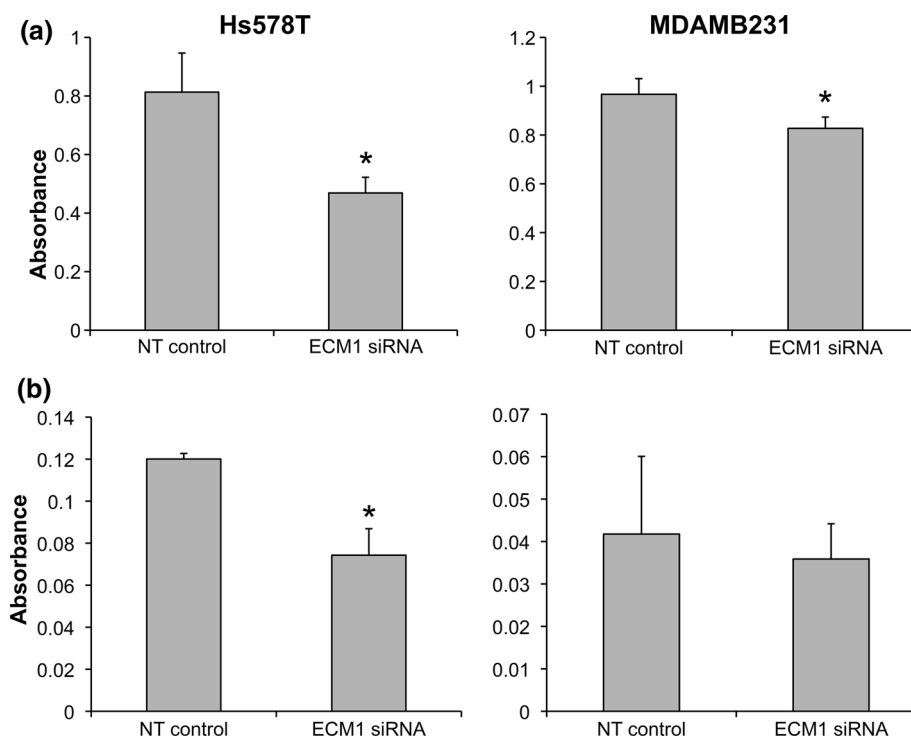


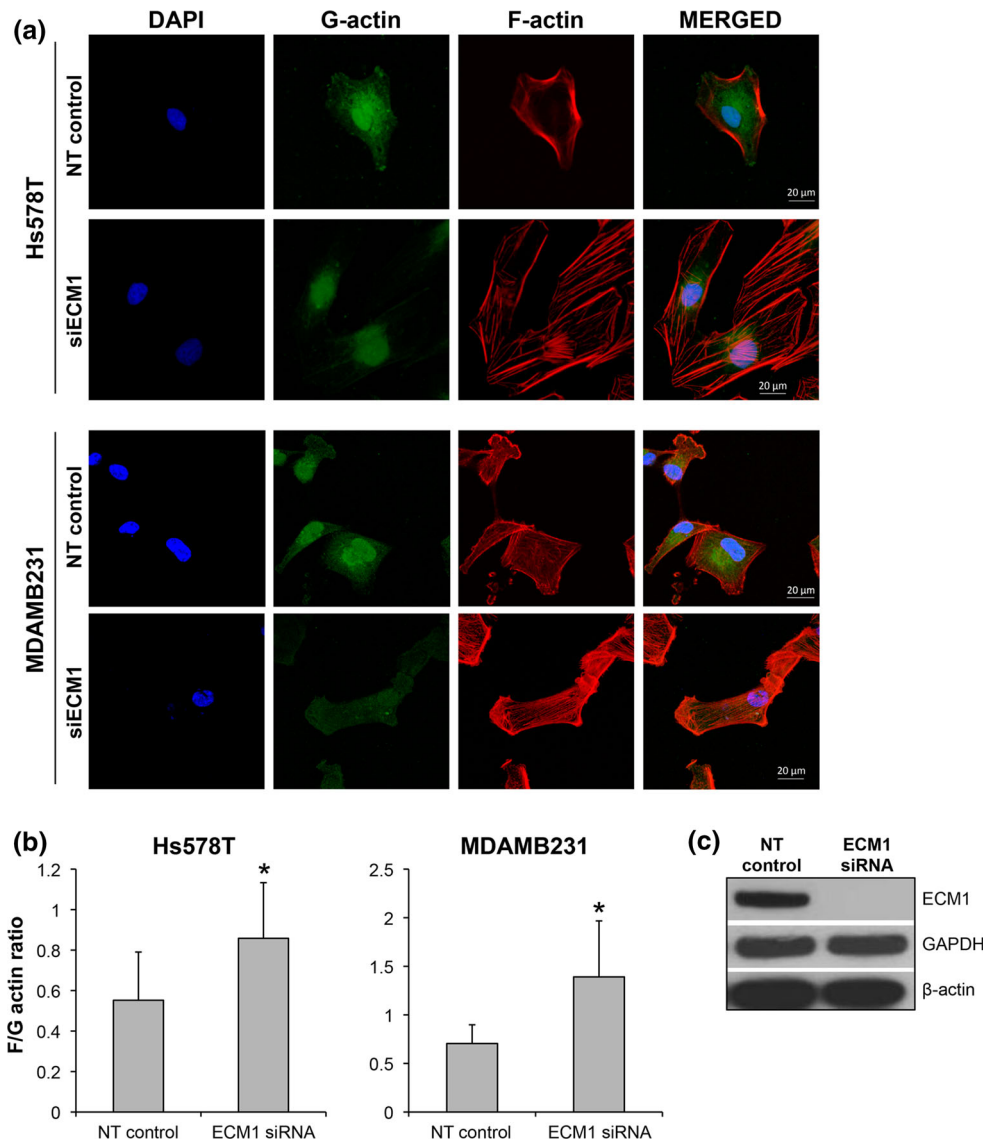
**Fig. 3** ECM1 silencing affects the expression of several metastasis-associated genes. A RT-PCR using a 94-gene tumor metastasis array (TaqMan) was performed to assess the effects of ECM1 downregulation in Hs578T cells (data not shown). A selection of genes with fourfold changes in expression were further evaluated by western blot. Genes with less than fourfold change in their RNA expression

The levels of F- and G-actin were also quantified. We found that ECM1 silencing increased F/G-actin ratio in both cell lines ( $p < 0.001$  for Hs578T and  $p < 0.0003$ ) for MDAMB231, when compared to cells transfected with

but known relevance to breast carcinogenesis were also evaluated in both cell lines. GAPDH expression was used as loading control for all westerns. **a** Representative blots are shown. **b** The westerns were repeated three times and densitometry data calculated. Error bars represent SD. \* $p < 0.05$

NT siRNA, Fig. 4b. Interestingly, as seen in Fig. 4c, despite ECM1 downregulation (>90%), total actin expression remains unchanged. This suggests that ECM1 likely affects the overall architecture of the cytoskeleton

**Fig. 4** ECM1 expression regulates cytoskeleton architecture. Loss of ECM1 was also associated with changes in the cellular shape, wherein ECM1 siRNA treated cells appeared more elongated and spindle shaped when compared to cells treated with NT siRNA. Changes in the cell cytoskeleton were evaluated using F-actin and G-actin staining. Nuclei were stained with DAPI. **a** ECM1 knockdown induces cytoskeleton rearrangement in both cell lines with decreased membrane ruffling and increase in the formation of stress fibers. **b** Significant increase in F/G-actin ratio was seen in both cell lines (\* $p < 0.01$ ) after 96 h of ECM1 silencing. Error bars represent SD of a sample of 12–15 cells. The figure shows results from one representative experiment. The experiments were repeated at least three times. **c** ECM1 silencing did not alter the total actin expression



through regulating the dynamics of the two forms of actin.

**Changes in the actin cytoskeleton are mediated by alteration in Rho A signaling**

Several cancers have been described to have elevated levels of Rho GTPases and high signaling activities [25]. Since Rho GTPases are the major effectors of changes to the actin cytoskeleton, we evaluated changes in these molecules. Rho A and Rho C are important players in the regulation of actomyosin contractility and cell movement, whereas Rho B has been shown to regulate intracellular trafficking and cell survival. Given that the role of Rho B in cancer progression in vivo is yet to be completely elucidated, we decided to focus our experiments on Rho A and Rho C, in addition to Cdc42 and Rac1.

ECM1 silencing did not lead to any changes in the expression levels of these proteins by western blot in Hs578T cell line (which shows more pronounced ECM1 expression). We therefore performed GST-pull-down assays for activities of these molecules. Cdc42 and Rac1 pull-down assays did not show consistent changes over two experiments and we thus did not pursue these analyses further.

As expected, there was high intrinsic activity of Rho A and Rho C in both the cell lines studied. In the representative western blots shown in Fig. 5a, activated Rho A was down-regulated, whereas activated Rho C did not show any significant changes. The pull-downs were repeated and comparison of the densitometry analyses over at least three experiments demonstrated a significant reduction in active Rho A in the Hs578T cell line ( $p = 0.05$ ). Rho A signaling was also diminished in the MDAMB231 cells although the results did not reach statistical significance ( $p = 0.1$ ) as seen in Fig. 5b.

## S100A4 is the likely effector for ECM1-related cytoskeletal changes

Since S100A4 can influence the delicate balance between Rho A-mediated actin polymerization and actomyosin contractility, and ECM1 silenced cells show reduction in S100A4 levels, we examined the effects of silencing S100A4 on the actin cytoskeleton structure of the cells. As shown in Fig. 6 cells transfected with siRNA S100A4 demonstrated loss of membrane ruffling and formation of stress fibers when compared to cells transfected with NT siRNA. Similar morphological changes were observed when an alternate siECM1 was used (targeting a different exon), along with a concomitant decrease in S100A4 expression. Of note, S100A4 silencing also significantly decreased wound migration in the MDAMB231 cell line compared to NT cells ( $p = 0.01$ ), however, there was no difference in percentage healed wound area between ECM1 and S100A4 silenced cells (Supplemental Figure 2). Taken together, these data suggest that the cytoskeletal alterations are unlikely an off-target effect of ECM1 and suggest that the effects of ECM1 may be mediated by direct reduction in S100A4 levels.

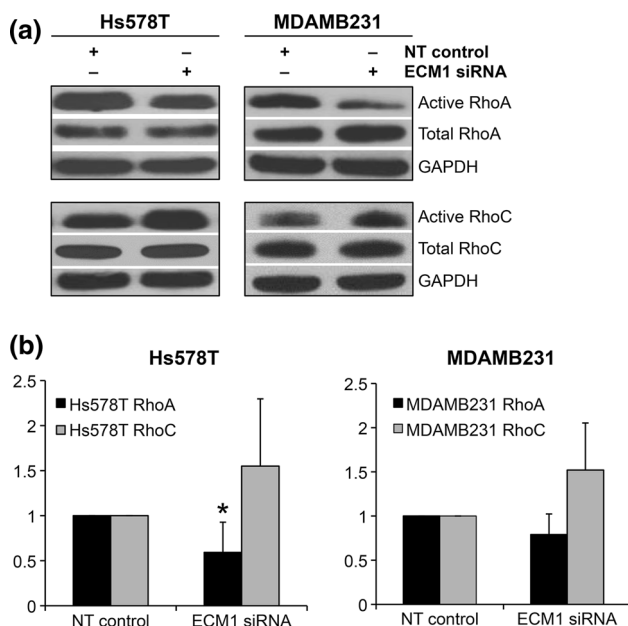


**Fig. 5** ECM1 knockdown alters Rho A activity. **a** Rho A and Rho C GTP active forms were evaluated by pull down assay in both cell lines. Blots represent one representative experiment. The samples were normalized to their NT controls. **b** Plots show the changes in active Rho A and Rho C as evaluated using the densitometry. NT controls were designated as 1. \* $p = 0.05$  for RhoA in Hs578T and  $p = 0.1$  in MDAMB231 respectively. Bars represent SD of densitometry from a least three pulldown assays. Levels of active Rho C did not change significantly

We then proceeded to re-express S100A4 in the ECM1 silenced cells to determine if this would rescue the phenotypic changes seen with ECM1 downregulation. Changes in the actin cytoskeleton seemed to revert in cells transfected with the S100A4 vector when compared to the cells transfected with the GFP-empty vector in both the cell lines as shown in Fig. 7a. We quantified the data by calculating the percentage of the pixels in each cell that were positive for F-actin in multiple cells from additional sets of experiments. As demonstrated in Fig. 7b, cells transfected with the vector containing S100A4 had significantly lower F-actin than those transfected with the empty vector ( $p = 0.008$ ) or non-transfected cells ( $p = 0.01$ ) in the HS578T cells. There was no difference in the cells transfected with the empty vector versus non-transfected cells. The changes in F-actin were not statistically significant in the MDAMB231 cells (S100A4 vs. empty vector,  $p = 0.17$ ), as seen in Fig. 7c.

## Discussion

ECM1 overexpression has been correlated with a poor prognosis in multiple malignancies, including breast cancers. However, studies investigating the mechanisms underlying this phenomenon are rather limited. Two recent reports have supported the hypothesis that ECM1 is involved in the regulation of breast tumor metastasis [13, 14]. Although Lee et al. [14] described reduction in S100A4 RNA levels, to the best of our knowledge, this is the first study exploring alterations in cell morphology, the actin cytoskeleton and subsequent effects on S100A4 protein expression and Rho GTPases as potential mechanisms by which ECM1 expression can affect prognosis in breast cancers. The demonstration that ECM1 expression can alter expression of other metastasis-associated genes like CD44 and TGF $\beta$ R2 is also novel.

In general, ER-negative breast tumors have a worse prognosis. In particular, triple negative tumors (ER-, PR- and Her2 negative) do very poorly. Of the multiple cell lines screened, only Hs578T and MDAMB231 were ECM1-positive. Hs578T is derived from a carcinoma-sarcoma primary breast tumor and MDAMB231 from a metastatic adenocarcinoma. Both cell lines have been previously characterized as triple-negative, with a basal-B subtype. They are highly invasive and characterized by features of epithelial-mesenchymal transition markers associated with aggressive tumor features, as well as marker phenotypes associated with normal breast and breast cancer progenitor/stem cells [26].

Downregulation of ECM1 expression resulted in alterations in cell migration, invasion, adhesion and morphology. Xiong et al. [6] also reported reduced cell migration



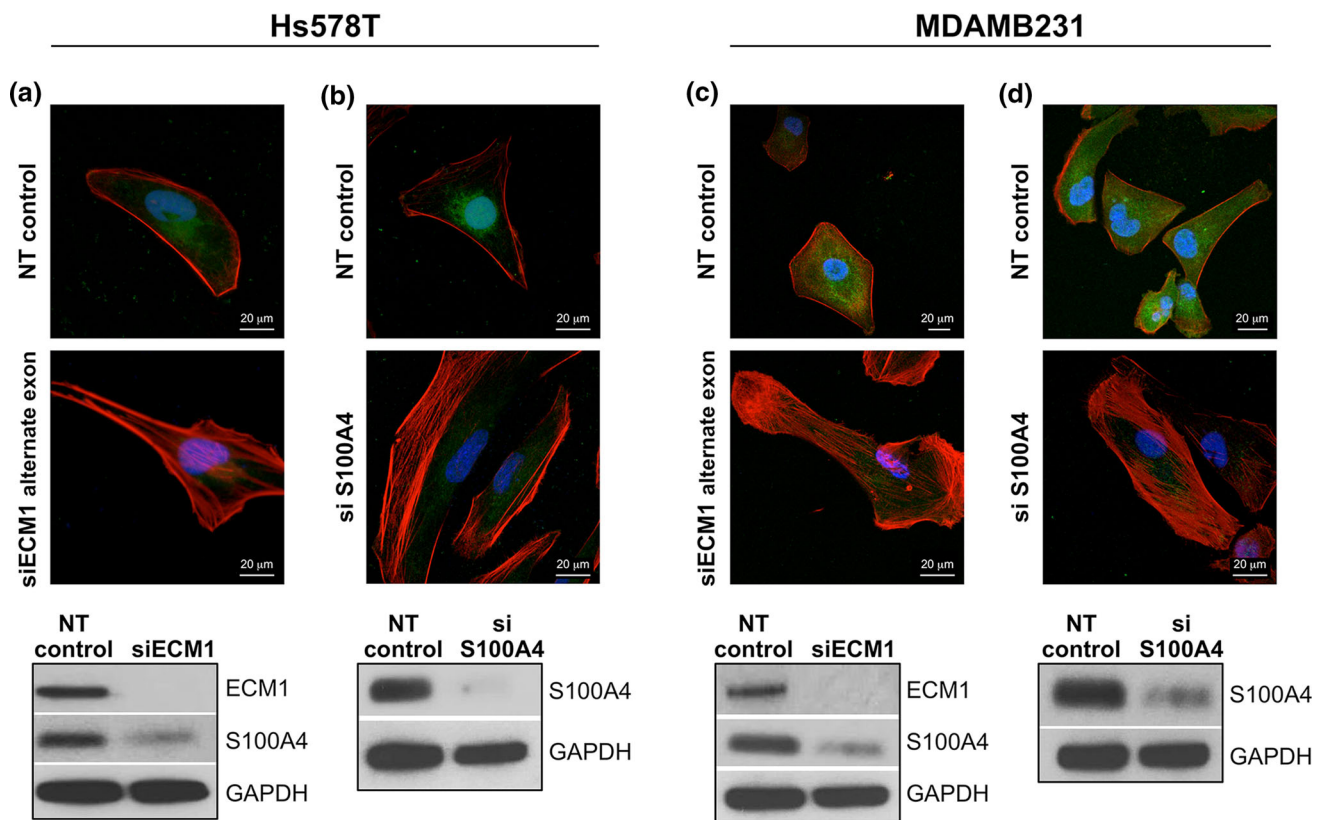


**Fig. 6** Changes in cellular cytoskeleton are ECM1 specific and may be related to altered levels of S100A4. **a, c** ECM1 was silenced in both cell lines using a different siRNA (alternate exon) and the cells showed similar morphological changes with increased stress fiber formation. ECM1 silencing was also associated with downregulation

of S100A4 levels. **b, d** Silencing S100A4 also leads to increased stress fiber formation. All immunofluorescence images are at  $\times 60$  magnification. Similar to Fig. 4, *blue* represents the nucleus, *red* represents F-actin and *green* represents G-actin. (Color figure online)

and invasion (through matrigel) in cholangiocarcinoma cell lines following ECM1 silencing. We have recently shown that ECM1 downregulation led to reduced adhesion of A375 and M21 melanoma cells in culture, although it did not affect cell migration or invasion [16]. In contrast, cell migration and attachment were the most consistently affected characteristics in the breast cancer cells. Our findings are also in keeping with those of Lee et al. [14] who reported that ECM1 affects both breast cancer cell line migration and invasion. While they also demonstrated that ECM1 can affect sphere-forming ability (a hallmark feature of CSCs), the effects of altering ECM1 on breast cancer cell morphology and adhesion have not been previously described.

Actin is a key protein involved in the changes observed in migratory cells during the metastatic process. It exists in two molecular forms—a globular (G-actin) and a polymerized filamentous (F-actin) form—which are continuously switching in the cell in a delicate and balanced equilibrium [27]. Aberrations in actin mechanics have also been implicated in cancer metastasis and invasion [28]. The Rho family of small GTPases belong to the Ras

superfamily and chiefly function to co-ordinate reorganization of the actin cytoskeleton (especially related to cell motility and invasion) in response to stimuli such as growth factors, cytokines and adhesion receptor activation [29]. Both Rho A and Rho C have shown high protein levels and significant signaling activity in breast cancers [30, 31].

We explored the actin distribution and activity of Rho A and C GTPases in our cell lines. MDAMB231 cells have previously been shown to have a constitutively active Rho A [32]. In earlier studies, Rho A has been reported to promote the formation of stress fibers and strong focal adhesion complexes and was therefore thought to be inhibitory to cell migration. However, more recent investigations have shown that Rho A is activated at the leading edge of migrating cells where it is implicated in membrane ruffling and lamellae formation, events that are important in driving cell motility (reviewed in [29]). Rho A mediates both actin polymerization and actomyosin contractility and the delicate balance of these activities is needed to form membrane ruffles and lamellae (more actin polymerization) or stress fibers (more contractility). The switching of these complex processes can be affected not only by levels of

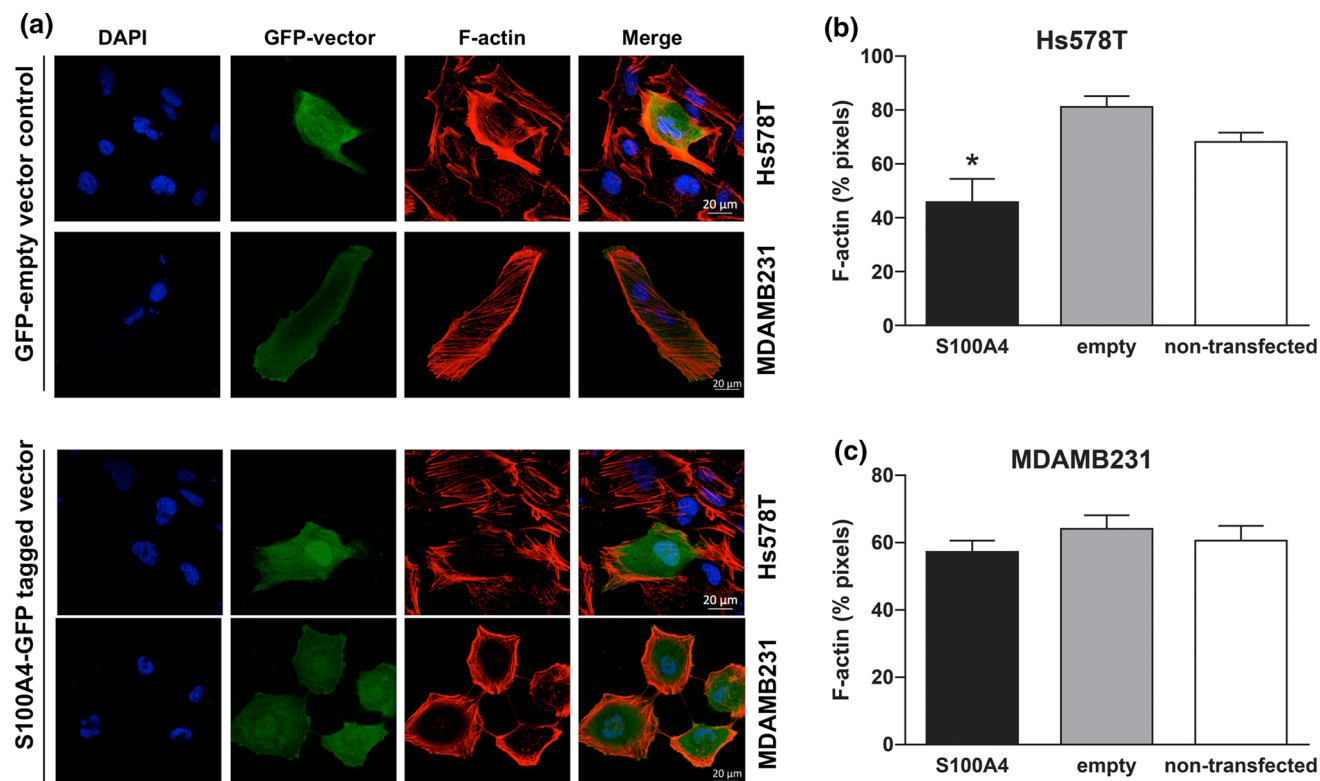


**Fig. 7** S100A4 rescues the phenotypic changes following ECM1 silencing. **a** A GFP empty vector control and an S100A4-GFP tagged vector were introduced into ECM1 silenced cells 48 h after silencing. Images were acquired at 96 h and show reduced F-actin stress fibers in cells transfected with S100A4 vector. **b, c** Quantification of F-actin.

\* $p < 0.05$ . Error bars represent SD of the number of cells analyzed over at least two experiments. All immunofluorescence images are at  $\times 60$  magnification. Blue represents the nucleus, red represents F-actin and green represents GFP. (Color figure online)

Rho A effectors such as ROCK and mDia, but also the prometastatic gene S100A4, a calcium binding EF hand protein. In cells expressing Rhotekin and S100A4, stimulation of Rho activity leads to coupling of Rho to S100A4. In this situation, myosin oligomerization is restricted in the proximity of active Rho thus limiting stress fiber formation. In the absence of S100A4 and Rhotekin, RhoA activation and non-oligomeric myosin do not co-localize, therefore the contractility events downstream of Rho A predominate, giving rise to stress fiber formation [33]. In keeping with this, both our motile cell lines transfected with NT siRNA demonstrated elevated Rho A activity and increased formation of lamellae/ruffling, whereas those transfected with siRNA-ECM1 demonstrated reduced Rho A activity and a predominance of stress fibers (demonstrated by phalloidin staining). On an interesting note, the NT siRNA cells also had elevated levels of S100A4 which was downregulated in ECM1-silenced cells, suggesting that S100A4 may function as the regulator of this switch in our cell lines. The fact that direct reduction of S100A4 levels in the cells via siRNA and downregulation of ECM1 using an alternate siRNA also led to increased stress fiber formation (and reduction of S100A4 levels in the latter) further lends

support to the model in which ECM1 mediates its effects via s100A4. As might be expected from the above, ECM1-silenced cells also showed an increase in F/G-actin ratio. The expression levels of  $\beta$ -actin were not altered, suggesting that the action of ECM1 is likely limited to dysregulation in the distribution of the proteins and thereby the overall cytoskeletal architecture. The changes in active Rho C were less consistent indicating that Rho A is most likely the key player in this process.

The changes observed in morphology, actin cytoskeleton, migration and Rho A activity are contrary to what would be expected. There might be a few explanations for this. With respect to phenotype and migration, various authors have shown that cell morphology changes induced by alterations in Rho A levels/activity do not always correlate with observed effects on migration/invasion and can also differ by cell line, long-term or short-term depletion or types of assays used. For example, Vega et al. [34] used siRNA to deplete Rho A in the MDAMB231 cell line and noted cell elongation on 2D substrata. The cells appeared to have reduced random migration speed, although chemotaxis was not affected. However, the cells seemed to invade more than control cells even though they also

appeared elongated in 3D strata. Similar to their findings, another group [35] reported that shRNA mediated Rho A depletion in SUM-159 cancer cells enhanced invasion. Rho A is known to act via ROCK1 and ROCK2 and their selective knockdown results in differing phenotypes and migration suggesting that the actions Rho A may be dependent on differences in downstream mediators [34]. Our additional studies demonstrated that, these differences may be due at least in part, to the presence S100A4, especially as increasing S100A4 expression in ECM1 silenced cells dramatically rescued the phenotype in the Hs578T cells. Of note, ECM1 expression is lower in MDAMB231 when compared to Hs578T cells and this may account for some of the less significant effects noted in the former cells [17]. In addition, the cytoskeletal changes in the MDAMB231 cells may be mediated by alternative pathways.

It is well known that a single gene or protein is unlikely to be the sole effector of the metastatic process. Knowledge regarding possible cooperation between metastasis-associated gene products and alterations of their functional activity is important to better our understanding of the process. As such, we noted that ECM1 does indeed appear to regulate the expression of various other genes known to be important in the metastatic process. These genes encompass various pathways and networks. Some are of known importance in breast cancer and others have known interactions with ECM1.

Aside from S100A4, TGF $\beta$ 2 was the other most dramatically downregulated gene in response to ECM1-silencing. Loss of expression or functional inactivation of TGF $\beta$ 1 or TGF $\beta$ 2 leads to resistance against TGF- $\beta$  [36, 37]. However, it appears that the ER status of tumor cells can influence the outcome of TGF $\beta$  effects as in other studies, expression of TGF $\beta$ 2 in primary tumors is correlated with a poor prognosis and represented an independent prognostic marker in ER-negative patients [38]. TGF $\beta$ 2 appeared to be expressed in both our tested ER-negative cell lines, and was downregulated in response to reduced ECM1 expression, indicating that ECM1 might also exert its effects on breast cancer cells via the TGF $\beta$  pathway. CD44 is a family of cell surface-transmembrane glycoproteins essential for maintaining cell adhesion and tissue integrity and its expression is related with the progression of many tumor types [39] including breast cancers, both in vitro and in vivo studies (reviewed in [40]). In fact, CD44 expression has been shown to contribute to breast cancer cell migration, invasion and adhesion [41]. In addition, CD44 is a stem cell marker in basal subtype breast cancer, and triple-negative tumors in particular. Downregulation of CD44 levels in response to ECM1-silencing in Hs578T cells lends further confirmation to the findings of other authors that have shown that ECM1 is

important in maintenance of the CSC phenotype and expression of genes related to “stemness”.

Despite the above findings, the mechanism by which ECM1 affects the expression of S100A4 and other genes remains to be determined. Given that ECM1 is a part of the extracellular matrix and is known to bind to other extracellular matrix components it is plausible the initial event downstream of ECM1 is likely mediated via the integrin signaling pathway. In fact, integrins are known to modulate breast cancer invasion via multiple pathways, [42] one of which involves signaling through Ras-PI3K to activate small GTPases in order to affect changes in the cytoskeleton. In addition, integrin  $\alpha$ 6 $\beta$ 4 is known to promote membrane ruffling and lamellae formation in breast carcinoma cells (mediated by Rho A) and also controls expression of S100A4. On the other hand one might speculate that changes in gene expression are mediated by changes in actin dynamics, which includes changes in G-actin and F-actin concentration. It is well known that changes in the cell cytoskeleton can promote changes at the transcription level via several pathways as reviewed by Olson and Nordheim [43]. Further elucidation of these mechanisms will be an important area of future study in our laboratory.

To summarize our findings, we demonstrate that ECM1 regulates not only several cellular characteristics and affects the expression of other metastasis-associated genes but also affects the actin cytoskeletal architecture of aggressive breast cancer cells. In addition, our data support a model in which ECM1 mediated changes in S100A4 expression may, at least in part, be the primary effector of these changes via alterations in the levels of Rho A expression. As such, we provide further evidence that ECM1 is a key component and possible regulator of the metastatic process. Initial investigations targeting ECM1 expression showed reduced lung metastases in a mouse model of breast cancer using MDAMB231 [14]. However, further studies are needed to determine which components of ECM1 mediated pathways can be targeted for an optimal response in patients with aggressive triple negative breast tumors with limited treatment options. These novel therapies will also have utility in the treatment of other poor-prognosis cancers overexpressing ECM1.

**Authors' contributions** P. Gomez-Contreras: concept, design of experiments, data acquisition, analysis and interpretation of data, writing of manuscript. J. M. Ramiro-Díaz: design of experiments, data acquisition, analysis and interpretation of data, writing of manuscript and critical review. A. Sierra: data acquisition, writing of manuscript draft. C. Stipp: concept and design, writing of manuscript and critical review. F. E. Domann: interpretation of data, critical review of manuscript. R. J. Weigel: concept, interpretation of data, critical review of manuscript. G. Lal: concept, design, data analysis and interpretation, writing of manuscript and critical review.

**Funding** This work was supported by NIH 1 K08 CA151658-01A1 (to GL) and the Department of Surgery at the University of Iowa. The funding sources have no role in the design of the study, data collection, analysis, interpretation of the data or writing of the manuscript.

#### Compliance with ethical standards

**Conflict of interest** The authors have no conflict of interest.

## References

- Wang L, Yu J, Ni J, Xu XM, Wang J, Ning H, Pei XF, Chen J, Yang S, Underhill CB et al (2003) Extracellular matrix protein 1 (ECM1) is over-expressed in malignant epithelial tumors. *Cancer Lett* 200(1):57–67
- Kebebew E, Peng M, Reiff E, Duh QY, Clark OH, McMillan A (2005) ECM1 and TMRSS4 are diagnostic markers of malignant thyroid neoplasms and improve the accuracy of fine needle aspiration biopsy. *Ann Surg* 242(3):353–361
- Lal G, Padmanabha L, Nicholson R, Smith BJ, Zhang L, Howe JR, Robinson RA, O'Dorisio MS (2008) ECM1 expression in thyroid tumors—A comparison of real-time RT-PCR and IHC. *J Surg Res* 149(1):62–68
- Han Z, Lin GJ, Chi FL, Wang SY, Huang JM, Liu HJ, Zhang LR (2008) The relationship between the extracellular matrix and the angiogenesis and metastasis of laryngeal carcinoma. *ORL J Otorhinolaryngol Relat Spec* 70(6):352–358
- Chen H, Jia WD, Li JS, Wang W, Xu GL, Ma JL, Ren WH, Ge YS, Yu JH, Liu WB et al (2011) Extracellular matrix protein 1, a novel prognostic factor, is associated with metastatic potential of hepatocellular carcinoma. *Med Oncol* 28(Suppl 1):S318–325
- Xiong GP, Zhang JX, Gu SP, Wu YB, Liu JF (2012) Overexpression of ECM1 contributes to migration and invasion in cholangiocarcinoma cell. *Neoplasma* 59(4):409–415
- Han Z, Ni J, Smits P, Underhill CB, Xie B, Chen Y, Liu N, Tylzanowski P, Parmelee D, Feng P et al (2001) Extracellular matrix protein 1 (ECM1) has angiogenic properties and is expressed by breast tumor cells. *FASEB J* 15(6):988–994
- Wu QW, She HQ, Liang J, Huang YF, Yang QM, Yang QL, Zhang ZM (2012) Expression and clinical significance of extracellular matrix protein 1 and vascular endothelial growth factor-C in lymphatic metastasis of human breast cancer. *BMC Cancer* 12:47
- Wu Q, Li X, Yang H, Lu C, You J, Zhang Z (2014) Extracellular matrix protein 1 is correlated to carcinogenesis and lymphatic metastasis of human gastric cancer. *World J Surg Oncol* 12:132
- Meng XY, Liu J, Lv F, Liu MQ, Wan JM (2015) Study on the correlation between extracellular matrix protein-1 and the growth, metastasis and angiogenesis of laryngeal carcinoma. *Asian Pac J Cancer Prev APJCP* 16(6):2313–2316
- Lal G, Hashimi S, Smith BJ, Lynch CF, Zhang L, Robinson RA, Weigel RJ (2009) Extracellular matrix 1 (ECM1) expression is a novel prognostic marker for poor long-term survival in breast cancer: a Hospital-based Cohort Study in Iowa. *Ann Surg Oncol* 16(8):2280–2287
- Sercu S, Poumay Y, Herphelin F, Liekens J, Beek L, Zwijsen A, Wessagowit V, Huylebroeck D, McGrath JA, Merregaert J (2007) Functional redundancy of extracellular matrix protein 1 in epidermal differentiation. *Br J Dermatol* 157(4):771–775
- Lee KM, Nam K, Oh S, Lim J, Kim YP, Lee J, Yu JH, Ahn SH, Kim SB, Noh DY et al (2014) Extracellular matrix protein 1 regulates cell proliferation and trastuzumab resistance through activation of epidermal growth factor-signaling. *Breast Cancer Res* 16(6):479
- Lee KM, Nam K, Oh S, Lim J, Kim RK, Shim D, Choi JH, Lee SJ, Yu JH, Lee JW et al (2015) ECM1 regulates tumor metastasis and CSC-like property through stabilization of  $\beta$ -catenin. *Oncogene* 34(50):6055–6065
- Sercu S, Zhang L, Merregaert J (2008) The extracellular matrix protein 1: its molecular interaction and implication in tumor progression. *Cancer Invest* 26(4):375–384
- Lal G, Contreras PG, Kulak M, Woodfield G, Bair T, Domann FE, Weigel RJ (2013) Human melanoma cells over-express extracellular matrix 1 (ECM1) which is regulated by TFAP2C. *Plos ONE* 8(9):e73953
- Lopez-Marure R, Contreras PG, Dillon JS (2011) Effects of dehydroepiandrosterone on proliferation, migration, and death of breast cancer cells. *Eur J Pharmacol* 660(2–3):268–274
- Geback T, Schulz MM, Koumoutsakos P, Detmar M (2009) TScratch: a novel and simple software tool for automated analysis of monolayer wound healing assays. *Biotechniques* 46(4):265–274
- Kim HR, Gallant C, Leavis PC, Gunst SJ, Morgan KG (2008) Cytoskeletal remodeling in differentiated vascular smooth muscle is actin isoform dependent and stimulus dependent. *Am J Physiol Cell Physiol* 295(3):C768–778
- Johnson JL, Winterwood N, DeMali KA, Stipp CS (2009) Tetraspanin CD151 regulates RhoA activation and the dynamic stability of carcinoma cell-cell contacts. *J Cell Sci* 122(Pt 13):2263–2273
- Yilmaz M, Christofori G (2010) Mechanisms of motility in metastasizing cells. *Mol Cancer Res* 8(5):629–642
- Vigorito E, Billadeu DD, Savoy D, McAdam S, Doody G, Fort P, Turner M (2003) RhoG regulates gene expression and the actin cytoskeleton in lymphocytes. *Oncogene* 22(3):330–342
- de Frutos S, Diaz JM, Nitta CH, Sherpa ML, Bosc LV (2011) Endothelin-1 contributes to increased NFATc3 activation by chronic hypoxia in pulmonary arteries. *Am J Physiol Cell Physiol* 301(2):C441–450
- Nemeth ZH, Deitch EA, Davidson MT, Szabo C, Vizi ES, Hasko G (2004) Disruption of the actin cytoskeleton results in nuclear factor- $\kappa$ B activation and inflammatory mediator production in cultured human intestinal epithelial cells. *J Cell Physiol* 200(1):71–81
- Parri M, Chiarugi P (2010) Rac and Rho GTPases in cancer cell motility control. *Cell Commun Signal* 8:23
- Kao J, Salari K, Bocanegra M, Choi YL, Girard L, Gandhi J, Kwei KA, Hernandez-Boussard T, Wang P, Gazdar AF et al (2009) Molecular profiling of breast cancer cell lines defines relevant tumor models and provides a resource for cancer gene discovery. *Plos ONE* 4(7):e6146
- Blanchoin L, Boujemaa-Paterski R, Sykes C, Plastino J (2014) Actin dynamics, architecture, and mechanics in cell motility. *Physiol Rev* 94(1):235–263
- Kumar S, Weaver VM (2009) Mechanics, malignancy, and metastasis: the force journey of a tumor cell. *Cancer Metastasis Rev* 28(1–2):113–127
- O'Connor K, Chen M (2013) Dynamic functions of RhoA in tumor cell migration and invasion. *Small GTPases* 4(3):141–147
- Fritz G, Just I, Kaina B (1999) Rho GTPases are over-expressed in human tumors. *Int J Cancer* 81(5):682–687
- van Golen KL, Davies S, Wu ZF, Wang Y, Bucana CD, Root H, Chandrasekharappa S, Strawderman M, Ethier SP, Merajver SD (1999) A novel putative low-affinity insulin-like growth factor-binding protein, LIBC (lost in inflammatory breast cancer), and RhoC GTPase correlate with the inflammatory breast cancer phenotype. *Clin Cancer Res* 5(9):2511–2519



32. Denoyelle C, Albanese P, Uzan G, Hong L, Vannier JP, Soria J, Soria C (2003) Molecular mechanism of the anti-cancer activity of cerivastatin, an inhibitor of HMG-CoA reductase, on aggressive human breast cancer cells. *Cell Signal* 15(3):327–338
33. Chen M, Bresnick AR, O'Connor KL (2013) Coupling S100A4 to Rhotekin alters Rho signaling output in breast cancer cells. *Oncogene* 32(32):3754–3764
34. Vega FM, Fruhwirth G, Ng T, Ridley AJ (2011) RhoA and RhoC have distinct roles in migration and invasion by acting through different targets. *J Cell Biol* 193(4):655–665
35. Simpson KJ, Dugan AS, Mercurio AM (2004) Functional analysis of the contribution of RhoA and RhoC GTPases to invasive breast carcinoma. *Cancer Res* 64(23):8694–8701
36. Kalkhoven E, Roelen BA, de Winter JP, Mummery CL, van den Eijnden-van Raaij AJ, van der Saag PT, van der Burg B (1995) Resistance to transforming growth factor beta and activin due to reduced receptor expression in human breast tumor cell lines. *Cell Growth Differ* 6(9):1151–1161
37. Laiho M, Weis MB, Massague J (1990) Concomitant loss of transforming growth factor (TGF)-beta receptor types I and II in TGF-beta-resistant cell mutants implicates both receptor types in signal transduction. *J Biol Chem* 265(30):18518–18524
38. Buck MB, Fritz P, Dippon J, Zugmaier G, Knabbe C (2004) Prognostic significance of transforming growth factor beta receptor II in estrogen receptor-negative breast cancer patients. *Clin Cancer Res* 10(2):491–498
39. Jothy S (2003) CD44 and its partners in metastasis. *Clin Exp Metastasis* 20(3):195–201
40. Louderbough JM, Schroeder JA (2011) Understanding the dual nature of CD44 in breast cancer progression. *Mol Cancer Res* 9(12):1573–1586
41. Afify A, Purnell P, Nguyen L (2009) Role of CD44s and CD44v6 on human breast cancer cell adhesion, migration, and invasion. *Exp Mol Pathol* 86(2):95–100
42. Li DM, Feng YM (2011) Signaling mechanism of cell adhesion molecules in breast cancer metastasis: potential therapeutic targets. *Breast Cancer Res Treat* 128(1):7–21
43. Olson EN, Nordheim A (2010) Linking actin dynamics and gene transcription to drive cellular motile functions. *Nat Rev Mol Cell Biol* 11(5):353–365